Journal of Power Sources 273 (2015) 580–583

Contents lists available at ScienceDirect

Journal of Power Sources

journal homepage: www.elsevier.com/locate/jpowsour

Short communication

Enhanced power generation of microbial fuel cell using manganese dioxide-coated anode in flow-through mode

Changyong Zhang, Peng Liang*, Yong Jiang, Xia Huang

State Key Joint Laboratory of Environment Simulation and Pollution Control, School of Environment, Tsinghua University, Beijing 100084, PR China

HIGHLIGHTS

- A novel capacitive anode was made by electrodepositing MnO_2 on carbon felt.
- The addition of MnO_2 increased the capacitance of the anode.
- The MFC's power density improved 24.7% with the capacitive anode.
- Flow-through mode decreased the mass transfer resistance by 41.4%.

ARTICLE INFO

Article history:
Received 15 May 2014
Received in revised form
19 September 2014
Accepted 20 September 2014
Available online 28 September 2014

Keywords:
Manganese dioxide
Capacitive anode
Electron transfer
Flow-through mode
Mass transfer
Microbial fuel cell

ABSTRACT

A novel anode is fabricated by electrodepositing manganese dioxide (MnO_2) on carbon felt to promote MFC's power production. Compared to the bare carbon felt anode, when the electrodeposition time increases to 60 min, the anode capacitance improves 46 times. The maximum power density of the MFC with the MnO_2-coated anode reaches 3580 ± 130 mW m^{-2}, 24.7% higher than that with the bare carbon felt anode (2870 mW m^{-2}). MnO_2 is believed to facilitate extracellular electron transfer and accordingly improve the power output. Three anode substrate circulation modes, i.e., flow-through, side-flow, and no-flow, are applied. Electrochemical impedance spectroscopy (EIS) tests reveal that flow-through mode decreases the anode mass transfer resistance by 41.4% compared to the no-flow mode and contributes to the MFC's power production improvement.

1. Introduction

Microbial fuel cell (MFC) is a promising device for organic matter degradation through catalytic reaction of electrogenic microorganism and simultaneous electricity generation without external energy input [1–4]. However, the power output of the MFC is still too low to drive most commercially available electronic devices [5]. Power generation of the MFC can be improved when accelerating the anode substrate oxidation, electron transfer, and mass transfer [6,7].

To promote the anode substrate oxidation and electron transfer, exploring effective anode material is of great importance since the anode is not only the carrier of the electrogenic bacteria but also the conductor of the electron [7]. A high-performance anode material should have the following characteristics, excellent conductivity, good chemical stability, strong bio-compatibility, large surface area, and low cost [8,9]. The most versatile anode material for MFCs is carbon (felt, cloth, paper, and fibers) [10]. Carbon materials have little electrocatalytic activity and thus modification of carbon material is the main approach to improve their performance [11,12]. Recent studies demonstrated that carbon anode modified by transition metal oxide delivered larger capacitance and accelerated the extracellular electron transfer from electrogenic microbes to the anode, thus promoting power generation of MFC [13,14]. Lv et al. found power density of the MFC with RuO_2 coated anode (3080 mW m^{-2}) increased 17 times compared to that with the bare anode (180 mW m^{-2}) [13]. However, the high cost of RuO_2 restricts its practical applications. Peng et al. prepared an anode by rolling Fe_3O_4 in activated carbon and increased the MFC's maximum power density by 22% [14]. But the anode fabricated by the rolling process is not suitable for designing large specific surface electrode for the biofilm adhesion. MnO_2 is a transition metal dioxide with high specific capacitance, low cost, abundant resource, and environmentally benignity [15,16]. In previous researches, MnO_2 was

* Corresponding author. Tel.: +86 10 62796790.
E-mail address: liangpeng@tsinghua.edu.cn (P. Liang).

http://dx.doi.org/10.1016/j.jpowsour.2014.09.129
0378-7753/

normally used as a cathode catalyst [17,18]. But all the characteristics of MnO_2 suggests it may be a potential pseudo-capacitive anode modifier, which has rarely been explored.

To enhance anode mass transfer, accelerating the substrate stirring speed or circulation flow rate was normally applied, as it was feasible to reduce the mass transfer resistance. However, the mass transfer resistance can't be further lowered when the stir speed or circulation rate reaches a certain level [19]. Several recent studies demonstrated that the anode substrate circulation modes can enormously affected the power generation of the MFC. Employing the flow-through mode, when the anode substrate was driven to flow through the porous anode, increased the availability of substrate inside the anode and promoted the protons to transport away from the biofilm [20]. But how the flow-through mode influences the internal resistance (especially the mass transfer resistance) has not been investigated.

In this study, different amount of MnO_2 particles were electrodeposited on the carbon felt surface. Specific capacitance and resistance of the freshly prepared MnO_2-coated carbon felts were examined. Two-chamber MFCs were constructed with the MnO_2-modified carbon felts as the anodes. Linear Sweep Voltammetry (LSV) was conducted to investigate power production of the MFCs and electrochemical impedance spectroscopy (EIS) was applied to detect internal resistance of the MFCs. Three operation modes, i.e., flow-though, side-flow and no-flow, were employed. The effects of different operation modes on mass transfer resistance were also investigated by electrochemical impedance spectroscopy (EIS).

2. Experimental material and method

2.1. MnO_2-coated anode preparation and tests

The anode substrate was a piece of carbon felt (Shanghai Qijie Carbon Co., Ltd.) with a dimension of 3.0 cm in diameter and 0.5 cm in thickness. A Ti sheet (5.0 cm × 1.0 cm × 0.1 cm) was attached to the carbon felt to connect the external circuit. Prior to the electrodeposition, the carbon felt was cleaned in hot H_2O_2 solution (10%, 90 °C) for 3 h, then hot HCl solution (10%, 90 °C) for 1 h, followed by thorough rinse with deionized water and dried at 60 °C. Electrodeposition of MnO_2 on the carbon felt was performed in a two-electrode electrochemical cell consisting of a working electrode (carbon felt), a counter electrode (Ti sheet), and the $MnAc_2$ (0.25 M) solution as the electrolyte (Fig. S1). A constant current of 30 mA controlled by an Autolab potentiostat (PGSTAT 128N, Metrohm Autolab, Netherlands) was applied as the power source of the electrodeposition. The amount of MnO_2 deposited on the carbon felt was determined by the electrodeposition time, i.e., 5 min, 20 min, and 60 min. The carbon felts with these different amount of MnO_2 were designated as ED5, ED20, and ED60, respectively. They were then rinsed thoroughly with deionized water and dried at 60 °C for 4 h.

2.2. MFC construction, inoculation and operation

Four two-chamber MFCs were constructed with four different carbon felts as the anodes, i.e., bare carbon felt, ED5, ED20, and ED60, namely B-MFC, ED5-MFC, ED20-MFC, and ED60-MFC, respectively. The liquid volume of anode and cathode chamber were 28 mL and 21 mL, respectively. Between the two chambers, a cation exchange membrane (CMI7000, Membranes International Inc., U.S.) was applied as a separator. The modified carbon felt anode was inserted in the middle of the anode chamber, separating it into two parts. The carbon brush was used as the cathode. The MFCs (duplicated reactors) were inoculated with mixed bacterial cultures collected from the effluent of acetate-fed MFCs operated for more than six months in our laboratory. The anolyte was prepared by dissolving 1.64 g sodium acetate (NaAc), 0.31 g NH_4Cl, 4.4 g KH_2PO_4, 3.4 g $K_2HPO_4 \cdot 3H_2O$, 0.1 g $CaCl_2 \cdot 2H_2O$ and 0.1 g $MgCl_2 \cdot 6H_2O$ in 1.0 L deionized water; whereas, the catholyte was prepared by dissolving 16.64 g potassium ferricyanide $K_3Fe(CN)_6$ in 1.0 L phosphate buffered solution (KH_2PO_4 4.4 g L^{-1}, $K_2HPO_4 \cdot 3H_2O$ 3.4 g L^{-1}) [21]. The anode substrate was replaced every three days to remove planktonic and dead cells. Experimental temperature was kept at 30 °C.

Three circulation modes, i.e., flow-through (FT), side-flow (SF), and no-flow (NF), were tested after the MFCs were inoculated and stably operated for six months (Fig. 1). In the FT mode, the anode substrate was driven to flow through the anode. In the SF mode, the substrate flowed only along the left side of the anode. In both FT and SF modes, the substrate flow rate was 6 mL min^{-1}, controlled by a peristaltic pump. In the NF mode, the substrate was not circulated. The external resistance was fixed at 500 Ω. All the experiments were done in flow-through mode unless otherwise specified.

2.3. Electrochemical analysis

The capacitances of four freshly prepared anodes, i.e., bare carbon felt, ED5, ED20, and ED60, were determined by applying galvanostatic charge–discharge test, which was performed at a current load of 5 mA within a potential range from −0.5 V to 0.4 V (CHI 660 A, ChenHua, China). The capacitance of the anode can be calculated as [22],

$$C = It/\Delta U \quad (1)$$

where C is the capacitance of the anode (F), I is the charge–discharge current (A), t is the discharge time (s) and ΔU is the potential window (V). The resistance of the anode were measured by a multimeter.

The voltage drop across the external resistor (R_e, Ω) was measured every 5 min using a data acquisition system (DAQ2213, ADLINK, Beijing, China). MFC's polarization and power density curves were obtained by running linear sweep voltammetry (LSV) at a scan rate of 1 mV s^{-1} after the MFC were inoculated for three months, when the MFC was connected to the Autolab potentiostat (PGSTAT 128N, Metrohm Autolab, Netherlands). During the LSV test, the cathode acted as the working electrode, and the anode served as both the reference and counter electrodes [23]. The power density can be calculated as $P = UI/A$, where U is the voltage drop across the MFC, I is the current, and A is the projected surface area of the anode ($A = 7$ cm^2).

Electrochemical impedance spectroscopy (EIS) tests were carried out with the Autolab potentiostat. During the EIS test, the two-electrode mode was adopted with the anode served as the working electrode and the cathode as the counter electrode and reference electrode [24]. To ensure the system's stability during the test, the EIS was performed under the working condition when the MFC was connected to a fixed external resistance of 500 Ω [25]. Sixty-one frequencies were tested, ranging from 100 kHz to 0.1 Hz with a sinusoidal excitation signal of 10 mV. The software used for data fitting was Zview3.1 from Scribner Associates Inc [19].

The component of the internal resistance was obtained by fitting the EIS data point (frequency, real part, imaginary part) according to the equivalent circuit (inserted in Fig. 4). In the equivalent circuit, R_s represents the solution resistance, including the anode solution, CEM and cathode solution resistances. R_{act} is the anode charge transfer resistance. Z_w is the anode Warburg impedance. A constant-phase element (CPE) is proposed to represent the

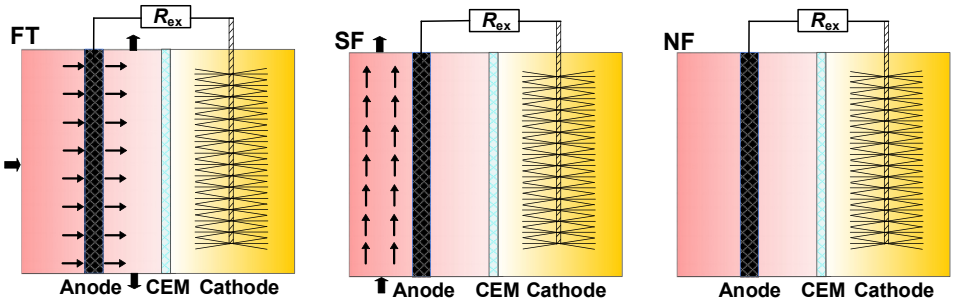

Fig. 1. Schematic diagram of three operation modes, i.e., FT, SF and NF.

electrical double layer capacitance, which is the result of charged electrolyte species accumulating near the charged surface of the electrode [26]. C_c and R_{cat} represent the cathode capacitance and cathode polarization resistance, including cathode charge and mass transfer resistance [27]. Since the EIS was performed at the working condition, an external resistance of 500 Ω was parallel connected to the MFC (designated as R_{ext} in the equivalent).

3. Results and discussion

3.1. Capacitance and resistance of the anode materials

The capacitance of the as-prepared anodes was investigated by performing the galvanostatic charge–discharge test. As shown in Fig. S1, the charge and discharge curves of the four anodes were all nearly linear and almost symmetrical, exhibiting excellent reversibility and capacitive property for these electrodes. The specific capacitance of the four anodes were calculated according to Equation (1) and illustrated in Fig. 2, as well as the specific resistances. The anode ED60 had the largest specific capacitance of 0.804 F cm^{-2}, 47 times of the bare carbon felt's (0.017 F cm^{-2}). However, the addition of MnO_2 increased the anode resistance as well. The specific resistance of the anode ED60 (2.67 Ω cm^{-2}) was much larger than that of the bare carbon felt (0.37 Ω cm^{-2}). Low electroconductivity of MnO_2 may be the major reason [16].

3.2. Electricity generation of MFCs with different anodes

During the first week of start-up period, the output voltages of ED60-MFC and ED20-MFC were much lower than those of ED5-MFC and B-MFC, mainly because that the relatively low electroconductivity of the MnO_2 restrained the initial enrichment of the bacteria. However, in the second and third week, the output voltages of ED60-MFC and ED20-MFC exceeded the ED5-MFC and B-MFC and achieved stability gradually (Fig. S3).

The polarization and power density curves of the four MFCs were shown in Fig. 3. The open circuit voltages (OCV) of the four MFCs had no remarkable difference (~0.72 V). The short-circuit current densities of the four MFCs were appreciably different. The B-MFC delivered the least short-circuit current density of 14.72 A m^{-2}, 27.3% less than the ED60-MFC (18.73 ± 1.12 A m^{-2}). The ED60-MFC produced a maximum power density of 3580 ± 130 mW m^{-2}, 24.7% higher than that of the B-MFC (2870 mW m^{-2}). The internal resistances were 82.5 and 65.1 Ω, for B-MFC and ED60-MFC, respectively. The Nyquist plots of the EIS were listed in Fig. S4. By fitting the data of the Nyquist plots using the Zview software, the value of each parameter was obtained (Table S1). The major parts of the internal resistance are solution resistance (R_s) and anode mass diffusion resistance (R_{ad}). The values of R_s of MFCs were quite similar. However, R_{ad} of ED60-MFC was 26.5 Ω, 34.1% lower than that of the B-MFC (40.2 Ω), indicating that the MnO_2-coated anode was capable of diffusing the substrate towards the electrode surface and improving the performance of the MFC.

The longer electrodeposition time resulted in larger amount of MnO_2 coated on the anode and higher anode capacitance (Fig. 2). Higher capacitance helps to stabilize the performance of anode and contribute to the power output [28]. It is also believed that MnO_2 could interact electrochemically with the bacteria and has the ability to facilitate extracellular electron transfer of the bio-electrochemical reactions.

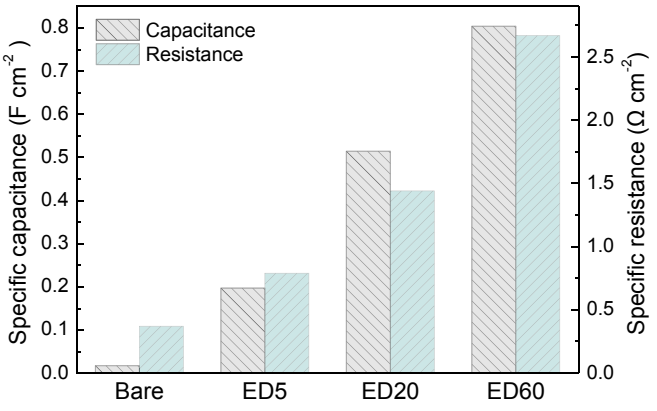

Fig. 2. Specific capacitance and specific resistance of the four anodes: Bare, ED5, ED20, and ED60.

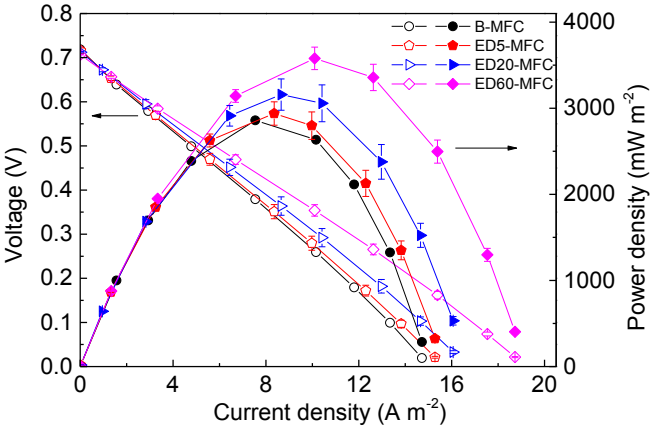

Fig. 3. Four MFC's power density curves (solid symbols) and polarization curves (open symbols).

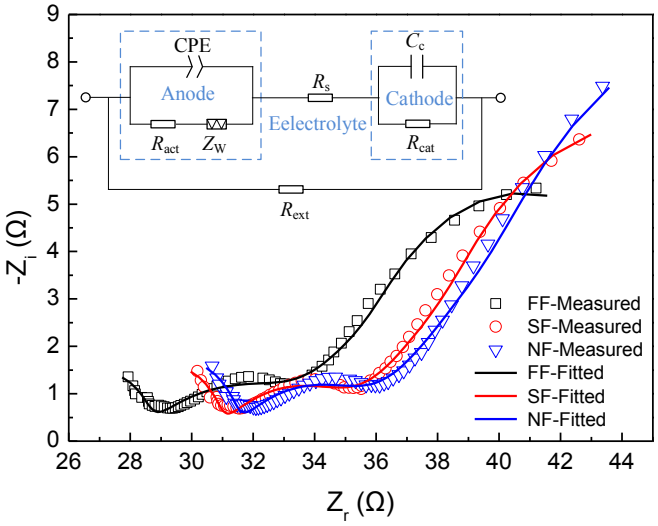

Fig. 4. Nyquist plots of impedance spectra by applying three operation modes (FT, SF and NF) and the fitted data (solid line) according to the equivalent circuit (inserted).

3.3. Operation mode test and EIS analysis

The ED60-MFC was selected for testing different operation modes, as it delivered the highest power production among all investigated MFCs. Three operation modes (FT, SF and NF) were tested as shown in Fig. 1. Each mode was operated until stable voltages was repeatedly produced. Then the EIS measurement was carried out to detect the internal resistance at the MFC's working condition with a fixed external resistance of 500 Ω.

Fig. 4 demonstrates the Nyquist plots and fitted plots (using the equivalent circuit described above) of the EIS measurements. Here, the horizontal axis is the real impedance ($Z_r(\Omega)$) and the vertical axis is the imaginary impedance ($-Z_i(\Omega)$). It can be seen that the fitted plots show the similar trends with the measured plots.

Each component of the internal resistance under different operation modes was fitted and illustrated in Fig. 5. Total internal resistances were 52.2, 58.1 and 65.3 Ω, at FT, SF and NF modes, respectively, indicating that the FT mode helped to reduce the total internal resistance. The difference of the total internal resistances was mainly attributed to the change of the anode mass diffusion resistances (R_{ad}). Applying FT mode enormously reduced the R_{ad} by

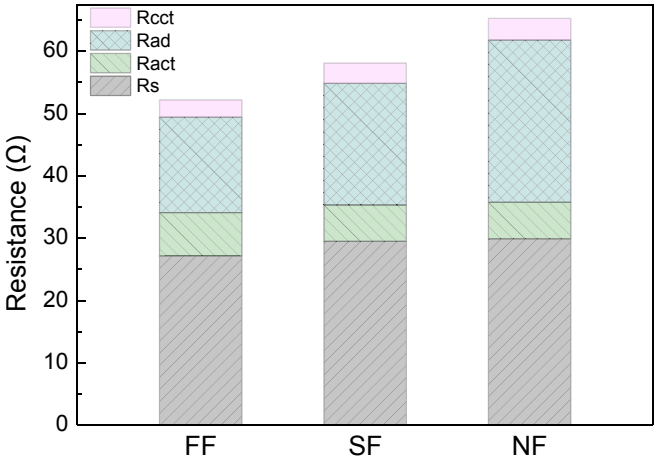

Fig. 5. Internal resistance distribution of the MFC operated at three operation modes.

21.9% and 41.4%, compared to the SF and NF mode. This result demonstrated that the FT mode enhanced the anode mass transfer and accordingly improved the MFC's power generation.

4. Conclusions

Carbon felt modified by manganese oxide was used as the anode of MFCs in this study. The MFC with the modified anode achieved a maximum power density of 3580 mW m^{-2}, 24.7% higher than that of MFC with bare carbon felt anode. The high specific surface area, pseudocapacitive behavior and good bio-compatibility contributed to the enhancement of electrode reaction and electron transfer. Flow-through mode could reduce the anode diffusion resistance by 41.4% and enhance the anode mass transfer compared to the no-flow mode. The adoption of the MnO_2-modified anode operated in flow-through mode improved the power generation of MFC.

Acknowledgments

This work was supported by the National Natural Science Foundation of China (NSFC No. 51278522), Tsinghua University Initiative Scientific Research Program (No. 20121087920), the Special Fund of State Key Joint Laboratory of Environment Simulation and Pollution Control (No. 13L03ESPC) and Program for Changjiang Scholars and Innovative Research Team in University.

Appendix A. Supplementary data

Supplementary data related to this article can be found at http://dx.doi.org/10.1016/j.jpowsour.2014.09.129.

References

[1] B.E. Logan, B. Hamelers, R. Rozendal, U. Schröder, J. Keller, S. Freguia, P. Aelterman, W. Verstraete, K. Rabaey, Environ. Sci. Technol. 40 (2006) 5181–5192.
[2] B.E. Logan, K. Rabaey, Science 337 (2012) 686–690.
[3] B.E. Logan, Nat. Rev. Microbiol. 7 (2009) 375–381.
[4] W.-W. Li, H.-Q. Yu, Z. He, Energy & Environ. Sci. 7 (2014) 911–924.
[5] D. Pant, A. Singh, G. Van Bogaert, S. Irving Olsen, P. Singh Nigam, L. Diels, K. Vanbroekhoven, RSC Adv. 2 (2012) 1248.
[6] A. ter Heijne, H.V.M. Hamelers, M. Saakes, C.J.N. Buisman, Electrochim. Acta 53 (2008) 5697–5703.
[7] Y. Qiao, C.M. Li, S.-J. Bao, Q.-L. Bao, J. Power Sources 170 (2007) 79–84.
[8] J. Wei, P. Liang, X. Huang, Bioresour. Technol. 102 (2011) 9335–9344.
[9] M. Zhou, M. Chi, J. Luo, H. He, T. Jin, J. Power Sources 196 (2011) 4427–4435.
[10] G.G. kumar, V.G. Sarathi, K.S. Nahm, Biosens. Bioelectron. 43 (2013) 461–475.
[11] H.-Y. Tsai, C.-C. Wu, C.-Y. Lee, E.P. Shih, J. Power Sources 194 (2009) 199–205.
[12] Z. Wen, S. Ci, S. Mao, S. Cui, G. Lu, K. Yu, S. Luo, Z. He, J. Chen, J. Power Sources 234 (2013) 100–106.
[13] Z. Lv, D. Xie, X. Yue, C. Feng, C. Wei, J. Power Sources 210 (2012) 26–31.
[14] X. Peng, H. Yu, X. Wang, Q. Zhou, S. Zhang, L. Geng, J. Sun, Z. Cai, Bioresour. Technol. 121 (2012) 450–453.
[15] G. Yu, X. Xie, L. Pan, Z. Bao, Y. Cui, Nano Energy 2 (2013) 213–234.
[16] C. Xu, F. Kang, B. Li, H. Du, J. Mater. Res. 25 (2011) 1421–1432.
[17] Y. Zhang, Y. Hu, S. Li, J. Sun, B. Hou, J. Power Sources 196 (2011) 9284–9289.
[18] L. Zhang, C. Liu, L. Zhuang, W. Li, S. Zhou, J. Zhang, Biosens. Bioelectron. 24 (2009) 2825–2829.
[19] A. Ter Heijne, O. Schaetzle, S. Gimenez, F. Fabregat-Santiago, J. Bisquert, D.P.B.T.B. Strik, F. Barrière, C.J.N. Buisman, H.V.M. Hamelers, Energy Environ. Sci. 4 (2011) 5035.
[20] T.H.J.A. Sleutels, R. Lodder, H.V.M. Hamelers, C.J.N. Buisman, Int. J. Hydrogen Energy 34 (2009) 9655–9661.
[21] L. Yuan, X. Yang, P. Liang, L. Wang, Z.H. Huang, J. Wei, X. Huang, Bioresour. Technol. 110 (2012) 735–738.
[22] Z. Lv, D. Xie, F. Li, Y. Hu, C. Wei, C. Feng, J. Power Sources 246 (2014) 642–649.
[23] Y. Yin, G. Huang, Y. Tong, Y. Liu, L. Zhang, J. Power Sources 237 (2013) 58–63.
[24] Z. He, N. Wagner, S.D. Minteer, L.T. Angenent, Environ. Sci. Technol. 40 (2006) 5212–5217.
[25] D. Aaron, C. Tsouris, C.Y. Hamilton, A.P. Borole, Energies 3 (2010) 592–606.
[26] A.P. Borole, D. Aaron, C.Y. Hamilton, C. Tsouris, Environ. Sci. Technol. 44 (2010) 2740–2745.
[27] Z. He, F. Mansfeld, Energy Environ. Sci. 2 (2009) 215.
[28] X. Peng, H. Yu, H. Yu, X. Wang, Bioresour. Technol. 138 (2013) 353–358.